

Kinetic roughening of surfaces: Derivation, solution and application of linear growth equations

S. Majaniemi¹, T. Ala-Nissila¹⁻³ and J. Krug⁴

¹Research Institute for Theoretical Physics
P.O. Box 9 (Siltavuorenpenger 20 C)
FIN-00014 University of Helsinki, Finland

²Department of Physics
P.O. Box 692
Tampere University of Technology
FIN-33101 Tampere, Finland

³Department of Physics
Box 1843
Brown University
Providence R. I. 02912, U.S.A.

⁴Institut für Festkörperforschung
Forschungszentrum Jülich
D-52425 Jülich, Germany

⁵Present address:
Fachbereich Physik, Universität GH Essen
D-45117 Essen, Germany

January 16, 1996

Abstract

We present a comprehensive analysis of a linear growth model, which combines the characteristic features of the Edwards–Wilkinson and noisy Mullins equations. This model can be derived from microscopics and it describes the relaxation and growth of surfaces under conditions where the nonlinearities can be neglected. We calculate in detail the surface width and various correlation functions characterizing the model. In particular, we study the crossover scaling of these functions between the two limits described by the combined equation. Also, we study the effect of colored and conserved noise on the growth exponents, and the effect of different initial conditions. The contribution of a rough substrate to the surface width is shown to decay universally as $w_i(0)(\xi_s/\xi(t))^{d/2}$, where $\xi(t) \sim t^{1/z}$ is the time-dependent correlation length associated with the growth process, $w_i(0)$ is the initial roughness and ξ_s the correlation length of the substrate roughness, and d is the surface dimensionality. As a second application, we compute the large distance asymptotics of the height correlation function and show that it differs qualitatively from the functional forms commonly used in the interpretation of scattering experiments.

PACS numbers: 68.55.-a, 68.10.Jy, 05.40.+j.

1 Introduction

The dynamics of interfaces ranging from dendritic growth to flame front propagation can often be described by relatively simple evolution equations [1]. Typically such evolution equations are given in terms of partial differential equations with a stochastic noise component. Perhaps the best known example is the nonlinear Kardar–Parisi–Zhang (KPZ) equation [2] which describes kinetic roughening of randomly driven interfaces such as growing surfaces or flame fronts in forest fires [3]. Complete understanding of these nonlinear equations is still mostly lacking.

Under certain circumstances discussed below the relevant nonlinearities may be so weak that a fully *linear* model can provide an adequate description. One example is the growth model of Edwards and Wilkinson (EW) [4], which describes the sedimentation of granular particles under gravitation. Another important model is the noisy Mullins equation discussed by Wolf and Villain and others [5, 6, 7] (the Mullins–Wolf–Villain (MWV) equation) in the context of molecular beam epitaxy (MBE). Being linear, both of these equations have been analyzed in some detail. However, recently it has been shown both from macroscopic arguments [8] and through more microscopic derivations [9, 10] that for some cases involving surface diffusion and desorption, a more general linear equation of the form

$$\partial_t h = \nu_1 \nabla^2 h + \nu_2 \nabla^4 h + \eta \quad (1)$$

emerges, where $h = h(\vec{x}, t)$ is the surface height above a d -dimensional substrate, $\eta(\vec{x}, t)$ is a noise term, and ν_1 and ν_2 are parameters. Since the gradient terms of Eq. (1) are simply a combination of the EW and MWV equations, we call it the *Combined Linear Growth* (CLG) equation. Stability requires that $\nu_1 \geq 0$ and $\nu_2 \leq 0$. While it is physically possible that $\nu_1 < 0$ (see Sec. 2.2), the treatment of this case requires the inclusion of additional nonlinear terms in (1), and will not be addressed here.

The purpose of the current work is to present a detailed analysis of Eq. (1), which is missing so far. This is useful for two main reasons. First, the calculations in this work generalize the previous results obtained for the EW and MWV equations which are somewhat incomplete and scattered in the literature [4, 5, 7, 8, 11, 12, 13, 14, 15, 16]. Second, Eq. (1) is the simplest example of a growth equation with an *intrinsic length scale*. Balancing the two gradient terms in (1) one finds that they become comparable at the scale

$$\ell^* = \sqrt{|\nu_2|/\nu_1}. \quad (2)$$

The kinetic roughening process is governed by the fourth derivative term on scales smaller than ℓ^* but the second order term dominates on scales larger than ℓ^* . Physically, the two terms represent different relaxation mechanisms, through surface diffusion (fourth derivative), evaporation–condensation or step edge barriers (second derivative) [8, 17]. Of course, writing a continuum equation with an intrinsic scale is meaningful only if this scale much exceeds the microscopic cutoff, given by the lattice spacing a ; the detailed estimated of ν_1 and ν_2 derived in Sec. 2 show that ℓ^* is indeed *mesoscopic*, in the sense that $\ell^* \gg a$, under typical conditions. Mesoscopic intrinsic length scales such as domain [18] or terrace [19] sizes play an important role in the kinetic roughening of real surfaces. Moreover, the competition and interplay between different relaxation and roughening mechanisms is probably typical in many experimental situations; for this reason combined linear equations like (1) have already been used extensively in the analysis of experimental data [20].

A major advantage of working with *linear* growth equations is that they allow us to explicitly compute any statistical quantity of interest, rather than just extracting the values of scaling exponents, which have been the focus of most previous studies of kinetic roughening [21]. We will exploit this fact to address two questions of direct experimental relevance: The evolution of the initial substrate roughness during growth, and the shape of the height–height correlation function. In both cases we find that the heuristic expressions commonly employed in the experimental literature are *incompatible* with the explicit calculations.

The organization of the paper is as follows. We shall first briefly review the physical background and various arguments leading to Eq. (1), and in particular various interpretations of the coefficients ν_1 and ν_2 . Following this, Sec. 3 contains a full solution of the CLG model in terms of the relevant measures of the surface roughness. We concentrate on the scaling behavior and finite size dependence of the surface width $w(L, t)$, the equal time height–height correlation function $G(x, t)$, and the saturated height–height correlation function $C_s(x, t)$. In particular, we study in detail the *crossover behavior* of these quantities to the well known limits given by the EW and MWV equations. In Sec. 4 we discuss the experimentally important effects of substrate roughness, the shape of the height correlation function and the influence of long ranged noise correlations. Finally, summary and conclusions are given in Sec. 5.

2 Derivation of the Linear Growth Model

In this section we provide some microscopic justification for the combined linear growth equation (1). We consider two different physical situations, corresponding to a surface in thermal equilibrium (Sec. 2.1) and a vicinal

surface growing in the step-flow mode (Sec. 2.2), respectively. In both cases the fourth order derivative term in (1) reflects capillarity-driven surface diffusion [17], while the second order term will be seen to arise from distinct mechanisms.

2.1 Equilibrium Dynamics of a Solid-on-Solid Model

We consider a one-dimensional solid-on-solid surface described by a set of integer height variables h_i defined on a lattice. The energy of the surface is given by the Hamiltonian [22]

$$\mathcal{H} = (K/2) \sum_i |h_i - h_{i+1}|. \quad (3)$$

The surface evolves according to the following dynamic processes [9]: Particles are deposited ($h_i \rightarrow h_i + 1$) at a constant rate F ; they evaporate ($h_i \rightarrow h_i - 1$) at rate

$$W_i^{\text{ev}} = k_0 \exp[-(E'_S + n_i E'_N)/k_B T] \quad (4)$$

and jump from site i to site $j = i \pm 1$ at rate

$$W_{ij}^{\text{diff}} = k_0 \exp[-(E_S + n_i E_N)/k_B T]. \quad (5)$$

Here k_0 defines some microscopic hopping rate of the order of a typical phonon frequency. We will generally measure time in units of k_0^{-1} , so that effectively $k_0 = 1$; likewise the basic length unit will be provided by the lattice constant. The energy barriers in (4) and (5) each have a substrate contribution (E'_S and E_S) and a bonding contribution proportional to the lateral coordination number

$$n_i = \theta(h_{i+1} - h_i) + \theta(h_{i-1} - h_i) \quad (6)$$

which takes the values $n_i = 0, 1, 2$ in one dimension. Detailed balance relative to (3) holds if

$$E_N = E'_N = K \quad \text{and} \quad F = k_0 \exp[-(E'_S + K)/k_B T]. \quad (7)$$

The distinguishing feature of the diffusion rates (5) is that they depend only on the environment at the initial site i . It was shown elsewhere [23] how this fact can be used to *exactly* derive the continuum equation of motion for the surface, in the case where only surface diffusion is allowed. Here we generalize the approach of [23] to include desorption and deposition. Note, however, that this derivation is only valid when the surface is in *equilibrium* with the vapor, as expressed by the second condition in (7).

From the master equation of the process one easily derives the following equation of motion for the ensemble averaged height [9, 23],

$$\frac{d}{dt} \langle h_i \rangle = \frac{1}{2} e^{-E_S/k_B T} (\nabla^2 \lambda)_i - e^{-E'_S/k_B T} \lambda_i + F \quad (8)$$

where $(\nabla^2 \lambda)_i = \lambda_{i+1} + \lambda_{i-1} - 2\lambda_i$ denotes the lattice Laplacian, and $\lambda_i \equiv \langle \exp[-(K/k_B T)n_i] \rangle$. This quantity is related to the local chemical potential μ_i [23],

$$\lambda_i = \exp[-(K - \mu_i)/k_B T]. \quad (9)$$

We now pass to the continuum limit $\langle h_i \rangle, \mu_i \rightarrow h(x, t), \mu(x, t)$, where $h(x, t)$ and $\mu(x, t)$ are averages taken over some large region (still small on the macroscopic scale) centered around $i = x$. The local chemical potential $\mu(x, t)$ is then determined by the local surface curvature via a Gibbs–Thomson relation

$$\mu = -\hat{\gamma}(\nabla h) \nabla^2 h \quad (10)$$

where the stiffness $\hat{\gamma}$ is a nonlinear function of the local surface slope that can be directly computed from the Hamiltonian (3) [23]; at zero tilt ($\nabla h = 0$)

$$\hat{\gamma}(0) = k_B T [\cosh(K/2k_B T) - 1]. \quad (11)$$

For slowly varying, macroscopic profiles the typical curvatures are small, so that (9) can be expanded in μ . This results in the macroscopic equation

$$\begin{aligned} \partial_t h = & -\frac{1}{2}(k_B T)^{-1} e^{-(E_S + K)/k_B T} \nabla^2 [\hat{\gamma}(\nabla h) \nabla^2 h] + \\ & + (k_B T)^{-1} e^{-(E'_S + K)/k_B T} \hat{\gamma}(\nabla h) \nabla^2 h \end{aligned} \quad (12)$$

which can be used e.g. to predict the decay of periodic surface modulations [23]. Note that the deposition term has disappeared due to the second of the detailed balance conditions (7). Because of the orientation dependence of the stiffness, (12) is highly nonlinear.

Here we are primarily interested in the mesoscopic fluctuations around a surface that is on average flat. Eq. (12) can then be linearized by expanding $\hat{\gamma}$ around the average orientation $u = \langle \nabla h \rangle$. It is not strictly speaking consistent to keep only the terms linear in h , since the nonlinearities arising from the expansion of the stiffness in the second term of (12) (such as $(\nabla h)^2 \nabla^2 h$) are more relevant in the renormalization group sense than the linear fourth order term; however we will ignore this difficulty in the interest of obtaining an analytically tractable model. Thus we arrive at the two systematic terms in (1), and identify the coefficients as

$$\nu_1 = (k_B T)^{-1} \hat{\gamma}(u) e^{-(E'_S + K)/k_B T}, \quad \nu_2 = -\frac{1}{2} (k_B T)^{-1} \hat{\gamma}(u) e^{-(E_S + K)/k_B T}. \quad (13)$$

To complete the derivation of (1), the statistics of the noise term has to be specified. This requires no further information, since detailed balance forces the stationary distribution of the continuum field $h(x, t)$ to be governed by the Hamiltonian

$$\mathcal{H}_c = (\hat{\gamma}(u)/2) \int dx (\nabla h)^2, \quad (14)$$

as can be seen from a central limit argument applied to the sum of independent local slope variables (3). A straightforward way to ensure the stationarity of $\exp[-\mathcal{H}_c/k_B T]$ is to modify the distribution functional of the white noise into the following form:

$$P[\eta] = \frac{e^{S[\eta]}}{Z}, \quad (15)$$

where $S = -(\hat{\gamma}(u)/2k_B T) \int dk \int dt (\nu_1 + \nu_2 k^2)^{-1} |\hat{\eta}(k, t)|^2$, and $Z = \int \mathcal{D}\eta e^{S[\eta]}$, where $\hat{\eta}(k, t)$ is the Fourier transform of $\eta(x, t)$. This leads to the noise covariance

$$\langle \eta(x, t) \eta(x', t') \rangle = 2(k_B T / \hat{\gamma}(u)) (\nu_1 + \nu_2 \nabla^2) \delta(x - x') \delta(t - t'). \quad (16)$$

Our derivation provides a microscopic basis for the classical theory of Mullins [17], who showed that second and fourth order derivatives of h arise from evaporation–condensation dynamics and surface diffusion dynamics, respectively. We may further conclude that the length scale beyond which the lower order derivative associated with evaporation–condensation dynamics dominates is given by

$$\ell^* \sim \sqrt{-\nu_2/\nu_1} \sim \exp[(1/2)(E'_S - E_S)/k_B T] \quad (17)$$

in units of the lattice constant. Since typically the activation energies for evaporation much exceed those for surface diffusion, ℓ^* can be quite large at moderate temperatures. It should be noted, however, that due to detailed balance the length scale (17) cannot appear in any stationary, equal time correlation functions, since these only depend on the Hamiltonian (14). Nevertheless, ℓ^* and a related time scale will appear in the time–dependent quantities, to be discussed in subsequent sections of this paper.

2.2 Step–Flow Growth on Vicinal Surfaces

Technologically important deposition techniques such as molecular beam epitaxy (MBE) are typically carried out at temperatures where desorption is negligible, so that effectively $\nu_1 = 0$ in (13). However, as was first pointed out by Villain [8], under growth conditions other mechanisms related to growth–induced surface currents [24] exist which generically give rise to a second order derivative in the continuum equation. A remarkable feature of such currents is that they can be destabilizing, leading to $\nu_1 < 0$ in (1). In the present work we focus on the kinetic roughening of a *stable* surface with $\nu_1 \geq 0$, and therefore we describe here only the simplest microscopic mechanism for the generation of a positive ν_1 term through the “Schwoebel” effect involving step edge barriers [25] (for some other mechanisms see [10]). As in the preceding section we restrict ourselves to a one dimensional surface. In two dimensions the mechanism described here gives rise to an anisotropic

Laplacian $\nu_{\parallel}\partial_{\parallel}^2 + \nu_{\perp}\partial_{\perp}^2$ in (1), with different coefficients ν_{\parallel} and ν_{\perp} parallel and perpendicular to the surface steps, at least one of which is negative [26]. We consider a *vicinal* surface with uniform step spacing ℓ , which is assumed to be much smaller than the diffusion length ℓ_D governing the island spacing on a *singular* surface [19]; this ensures that island nucleation on the terraces can be neglected, and the surface grows in the step flow mode [26]. Moreover we assume strong step edge barriers which effectively suppress any interlayer transport. Under such conditions every atom that is deposited on a terrace attaches to the ascending step edge, and the surface current is simply $J = F\ell/2$ (as before, F denotes the deposition rate) [8, 24, 26]. The coefficient ν_1 is then given by the negative derivative of J with respect to the surface inclination $1/\ell$ [24]. This yields

$$\nu_1 = F\ell^2/2. \quad (18)$$

Provided the capillarity-driven surface diffusion is not too strongly affected by the deposition, the expression (13) for ν_2 is still expected to be valid. Thus the crossover length scale (2) can be estimated as

$$\ell^* \sim \ell^{-1} \sqrt{-\nu_2/F} \sim \ell_{\text{cap}}^2/\ell \quad (19)$$

where $\ell_{\text{cap}} \sim (-\nu_2/F)^{1/4}$ is a length scale gauging the relative importance of capillarity and deposition [26]. For an order of magnitude estimate, we note that ν_2 can be directly measured from the decay time of periodically modulated surface profiles. For semiconductor surfaces a typical value is [27] $-\nu_2 \approx 1(\mu\text{m})^4$ per hour, implying that $\ell_{\text{cap}} \approx 1000 \text{ \AA}$ at a deposition rate of 1 s^{-1} . This much exceeds the step spacing on typical vicinal surfaces, and thus, as in the case of equilibrium dynamics (Sec. 2.1), there are good reasons to expect ℓ^* to be large compared to the lattice constant.

Of course, the most prominent effect of deposition is to provide an additional source of “shot noise” fluctuations. Assuming, again, that the (volume conserving) fluctuations due to surface diffusion are not much changed by the deposition flux, we obtain the noise covariance

$$\langle \eta(x, t) \eta(x', t') \rangle = [F + 2(k_B T \nu_2 / \hat{\gamma}) \nabla^2] \delta(x - x') \delta(t - t'). \quad (20)$$

A comparison between the strengths of the two components of the noise, i.e. F and $k_B T \nu_2 / \hat{\gamma}$, defines a further crossover length scale

$$\ell^{**} \sim (D_{\text{coll}}/F)^{1/2} \quad (21)$$

where $D_{\text{coll}} = k_0 \exp[-(E_S + K)/k_B T]$ defines, within the present model, the *collective* surface diffusion coefficient [23]. In contrast to the detailed balance situation of Sec. 2.1, here the two crossover lengths ℓ^* and ℓ^{**} need not be equal. Their ratio is of the order

$$\ell^*/\ell^{**} \sim (k_B T)^{-1} \ell^{-1} \hat{\gamma}^{1/2} \sim \ell^{-1} \exp(K/4k_B T) \quad (22)$$

where in the last step we have used the expression (11) for small T . Thus, at low temperatures $\ell^* \gg \ell^{**}$. This provides some justification for neglecting the conserved noise component in (20), as will be done throughout Sec. 3.

3 Solutions for Various Physical Quantities

In this section we summarize our results for the physically interesting measures of the surface roughness of the CLG model, for arbitrary surface dimensionalities $d \leq z$, where z is the dynamic exponent. The physically interesting quantities that we calculate are the surface width $w(L, t)$ and two correlation functions $G(\vec{x}, t)$ and $C_s(\vec{x}, t)$. The surface width is the size of typical height fluctuations around the mean $\bar{h} \equiv \langle \langle h(\vec{x}, t) \rangle_x \rangle_\eta$:

$$w^2(L, t) \equiv \langle \langle (h(\vec{x}, t) - \bar{h})^2 \rangle_x \rangle_\eta, \quad (23)$$

where $\langle \cdot \rangle_x$ and $\langle \cdot \rangle_\eta$ denote averaging over space and noise, respectively, and L is the lateral extent of the surface, assuming periodic boundary conditions. The two correlation functions can be derived from the general two point correlation function $C_g(\vec{x}, t, t')$, which is defined as:

$$C_g(\vec{x}, t, t') \equiv \langle \langle (h(\vec{x} + \vec{x}', t + t') - h(\vec{x}', t'))^2 \rangle_{x'} \rangle_\eta = C_g(x, t, t'). \quad (24)$$

All the correlation functions appearing in this section are thus dependent only on the magnitude $x = |\vec{x}|$. The equal time correlation function $G(x, t') \equiv C_g(x, t = 0, t')$ and the saturated correlation function $C_s(x, t) \equiv C_g(x, t, t' \gg t_s)$, where t_s is the saturation time to be defined later. We point out that the translational invariance of Eq. (1) makes the averaging over noise and space interchangeable when the noise correlations are also translationally invariant. In this section we assume Gaussian white noise of the form

$$\langle \eta(\vec{x}, t) \eta(\vec{x}', t') \rangle_\eta = 2D \delta^d(\vec{x} - \vec{x}') \delta(t - t') \quad (25)$$

$$\langle \eta(\vec{x}, t) \rangle_\eta = 0. \quad (26)$$

Later on in Sec. 4 we discuss the influence of the conserved noise component that appears in Eqs. (16) and (20). Here we also assume a flat initial condition, $h(\vec{x}, t = 0) = 0$. Growth on an initially rough surface is dealt with in Sec. 4.

The results for the CLG equation trivially reduce to the limits of the EW or MWV equations when $\nu_2 = 0$ or $\nu_1 = 0$, respectively. Also, simple power counting shows that for an *infinite* system, the EW behavior will always eventually dominate. In this work, however, we are interested in investigating the crossover time t_c from MWV to EW growth. The crossover always occurs for an *infinitely* large system where the MWV behavior is dominant for early times ($t \ll t_c$). Moreover, in a *finite* system for a suitable choice of the crossover length scale ℓ^* , the MWV growth can be made dominant for

all times. As was noted already, we focus on the stable case $\nu_1 > 0$, $\nu_2 < 0$. If $\nu_1 < 0$, the early time growth can be of MWV type but the long time behavior of the surface is unstable.

The main results for the CLG growth equation are given in the subsequent paragraphs. As usual [21], the asymptotics of the surface correlations involve the roughness exponent χ , the dynamic exponent z and the exponent ratio $\beta = \chi/z$ which describes how the surface width increases with time. The two limiting cases of (1) are characterized by the exponents

$$z_1 = 2, \quad \beta_1 = (2 - d)/4, \quad \chi_1 = (2 - d)/2 \quad (\text{EW}) \quad (27)$$

as was first derived in [4, 11], and

$$z_2 = 4, \quad \beta_2 = (4 - d)/8, \quad \chi_2 = (4 - d)/2 \quad (\text{MWV}), \quad (28)$$

compare to [5, 6, 7, 12]. It is understood that $\beta = \chi = 0$ implies logarithmic roughening.

The crossover time scale is given by $t_c = |\nu_2|/\nu_1^2$ and the saturation time (for finite system size L) by $t_s = L^{z_2}/(L^{z_1}\nu_1 + |\nu_2|)$. The crossover length scale $\ell^* = \sqrt{|\nu_2|/\nu_1}$ was defined in Sec. 1. In the following we use the dimensionless scaling variables: $p_1 \equiv \nu_1 t/L^2$, $p_2 \equiv |\nu_2|t/L^4$, $y_1 \equiv \nu_1 t/x^2$ and $y_2 \equiv |\nu_2|t/x^4$. The dynamic correlation lengths for the EW and MWV cases are defined as $\xi_1 \equiv (2\nu_1 t)^{1/2}$ and $\xi_2 \equiv (2|\nu_2|t)^{1/4}$.

3.1 Surface Width

The scaling function for the *surface width* is obtained from Eq. (23):

$$w^2(L, t) = \frac{2D}{\nu_1} L^{2\chi_1} F_w^1(p_1, p_2) = \frac{2D}{|\nu_2|} L^{2\chi_2} F_w^2(p_1, p_2), \quad (29)$$

where

$$F_w^j(p_1, p_2) = \frac{\Omega_{d-1}}{2(2\pi)^d} \int_1^\infty dk k^{d-1} [1 - e^{-2(p_1 k^2 + p_2 k^4)}] \frac{p_j}{p_1 k^2 + p_2 k^4}, \quad (30)$$

where Ω_{d-1} is the surface area of a d dimensional sphere, and $j = 1, 2$. We obtain the following power law behavior in the different time regimes:

If $p_1 \gg p_2$, then

$$w^2 \propto \begin{cases} L^{2\chi_1}, & \text{for } t \gg t_s; \\ t^{2\beta_1}, & \text{for } t_c \ll t \ll t_s; \\ t^{2\beta_2}, & \text{for } t \ll t_c. \end{cases} \quad (31)$$

If $p_1 \ll p_2$ then

$$w^2 \propto \begin{cases} L^{2\chi_2}, & \text{for } t \gg t_s; \\ t^{2\beta_2}, & \text{for } t \ll t_s. \end{cases}$$

The main result here is that for a *finite* system the MWV behavior can dominate for all times, including the saturated regime. This is shown in Fig. 1, where it can be seen that even for $p_1 = p_2$, the EW region can be made to vanish by choosing $t_s = t_c$.

3.2 Equal Time Correlation Function

The scaling function for the *equal time correlation function* is obtained from Eq. (24). Hence,

$$G(x, t) = \frac{2D}{\nu_1} x^{2\chi_1} F_G^1(y_1, y_2) = \frac{2D}{|\nu_2|} x^{2\chi_2} F_G^2(y_1, y_2), \quad (32)$$

where

$$F_G^j(y_1, y_2) = \frac{1}{(2\pi)^d} \int_{\Omega} \int_0^{\infty} dk k^{d-1} [1 - e^{-2(y_1 k^2 + y_2 k^4)}] [1 - \cos(k\alpha)] \frac{y_j}{y_1 k^2 + y_2 k^4}, \quad (33)$$

and $j = 1, 2$. The notation \int_{Ω} means angular integration, and $\alpha \equiv \cos(\vec{k}, \vec{x})$. We obtain the following power law behavior in the different regimes:

If $p_1 \gg p_2$ then

$$G(x, t) \propto \begin{cases} L^{2\chi_1}, & \text{for } x = \mathcal{O}(L) \text{ and } t \gg t_s; \\ x^{2\chi_1}, & \text{for } \ell^* \ll x \ll L \text{ and } t \gg t_s; \\ x^{2\chi_2} (L/x)^{2\chi_1}, & \text{for } x \ll \ell^* \ll L \text{ and } t \gg t_s; \\ x^{2\chi_1}, & \text{for } \xi_1 \gg x \gg \ell^* \text{ and } t_c \ll t \ll t_s; \\ t^{2\beta_1}, & \text{for } \ell^* \ll \xi_1 \ll x \text{ and } t_c \ll t \ll t_s; \\ x^{2\chi_2} (\xi_2/x)^{2\chi_1}, & \text{for } x \ll \xi_2 \ll \ell^* \text{ and } t \ll t_c; \\ t^{2\beta_2}, & \text{for } x \gg \xi_2 \text{ and } t \ll t_c. \end{cases}$$

If $p_1 \ll p_2$ then

$$G(x, t) \propto \begin{cases} L^{2\chi_2}, & \text{for } x = \mathcal{O}(L) \text{ and } t \gg t_s; \\ x^{2\chi_2} (L/x)^{2\chi_1}, & \text{for } x \ll L \text{ and } t \gg t_s; \\ x^{2\chi_2} (\xi_2/x)^{2\chi_1}, & \text{for } x \ll \xi_2 \text{ and } t \ll t_s; \\ t^{2\beta_2}, & \text{for } x \gg \xi_2 \text{ and } t \ll t_s. \end{cases} \quad (34)$$

To summarize, the correlation function can exhibit both EW and MWV scaling behavior for $p_1 \gg p_2$, while in the opposite case we find “anomalous” scaling behavior

$$G \sim x^{2\chi_2} (L/x)^{2\chi_1}, \quad G \sim x^{2\chi_2} (\xi_2/x)^{2\chi_1} \quad (35)$$

of the kind characteristic of the MWV equation [14] as well as certain non-linear models [15, 28, 29]. The scaling (35) is anomalous in the sense that G at fixed x has no finite limit for $L \rightarrow \infty$ and $\xi_2 \rightarrow \infty$; this implies the appearance of arbitrarily large height gradients and is associated with the

fact that the MWV roughness exponent $\chi_2 > 1$ for $d < 2$, compare to (28). Note that the increase of G with x in (35) is governed neither by χ_1 nor by χ_2 , but by an anomalous roughness exponent $\tilde{\chi} = \chi_2 - \chi_1 = 1$.

3.3 Saturated Correlation Function

The scaling function for the *saturated correlation function* is obtained from Eq. (24). Hence,

$$C_s(x, t) = \frac{2D}{\nu_1} x^{2\chi_1} F_C^1(y_1, y_2) = \frac{2D}{|\nu_2|} x^{2\chi_2} F_C^2(y_1, y_2) , \quad (36)$$

where

$$F_C^j(y_1, y_2) = \frac{1}{(2\pi)^d} \int_{\Omega} \int_0^{\infty} dk k^{d-1} [1 - e^{-(y_1 k^2 + y_2 k^4)} \cos(k\alpha)] \frac{y_j}{y_1 k^2 + y_2 k^4} , \quad (37)$$

and $j = 1, 2$. For simplicity, we only give the results in the limits where either $t = 0$ or $x = 0$. In the first case, the power law behavior of $C_s(x, 0)$ is given by:

If $p_1 \gg p_2$ then

$$C_s(x, 0) \propto \begin{cases} L^{2\chi_1} , & \text{for } x = \mathcal{O}(L); \\ x^{2\chi_1} , & \text{for } \ell^* \ll x \ll L; \\ x^{2\chi_2} (L/x)^{2\chi_1} , & \text{for } x \ll \ell^* \ll L. \end{cases} \quad (38)$$

If $p_1 \ll p_2$ then

$$C_s(x, 0) \propto \begin{cases} L^{2\chi_2} , & \text{for } x = \mathcal{O}(L); \\ x^{2\chi_2} (L/x)^{2\chi_1} , & \text{for } x \ll L. \end{cases}$$

The behavior of $C_s(0, t)$ is given by:

If $p_1 \gg p_2$ then

$$C_s(0, t) \propto \begin{cases} L^{2\chi_1} , & \text{for } t \gg t_s; \\ t^{2\beta_1} , & \text{for } t_c \ll t \ll t_s; \\ t^{2\beta_2} , & \text{for } t \ll t_c. \end{cases} \quad (39)$$

If $p_1 \ll p_2$ then

$$C_s(0, t) \propto \begin{cases} L^{2\chi_2} , & \text{for } t \gg t_s; \\ t^{2\beta_2} , & \text{for } t \ll t_s. \end{cases}$$

As in Sec. 3.2, both EW and MWV behavior are found in the different regimes.

4 Applications

The goal of the present section is to illustrate how linear growth equations can be used to address experimentally relevant questions about kinetic

roughening that have so far received little or no theoretical attention. Specifically, we discuss the contribution of the substrate roughness to the width of a growing surface, and the detailed form of the spatial height correlation function.

4.1 Effects of Substrate Roughness

In the real world, thin films are rarely deposited onto a perfect, atomically flat substrate. Consequently every experimental investigation of kinetic roughening has to deal with the substrate contribution to the roughness of the film surface. To the extent that this problem has been addressed at all, it is usually assumed [30] that the substrate gives an additive, constant contribution to the variance of the height fluctuations (the square of the width), as

$$w^2(t) = w_i^2 + w_G^2(t) \quad (40)$$

where w_i is the width of the substrate surface and w_G denotes the growth induced contribution (throughout this section the lateral system size is taken to be infinite and therefore the dependence on L is suppressed). This simple ansatz ignores the fact that the memory of the initial roughness is lost during the growth process, as the growing film successively covers up the features of the substrate. The short wavelength features are preferentially suppressed (compare to a layer of snow covering a rugged landscape), an effect of much importance for the scattering from multilayer films [31].

In the following we show that (i) within the framework of linear growth equations, the superposition ansatz (40) is justified, however (ii) the substrate contribution w_i becomes time dependent and decreases with t in a manner governed by the ratio of the substrate correlation length ξ_s to the correlation length $\xi(t) \sim t^{1/z}$ of the growth process; for long times, $\xi \gg \xi_s$, we find

$$w_i(t) \sim w_i(0)(\xi_s/\xi)^{d/2}. \quad (41)$$

The fact that the total width is the sum of a decreasing and an increasing part entails the somewhat counterintuitive possibility that $w(t)$ may initially *decrease* with increasing film thickness, as has been observed in recent experiments [32, 33].

To justify statements (i) and (ii), we assume that the surface has been grown from time $t = -t_0$ to $t = 0$ driven by some initial noise η_- in such a way that the height-height correlation function is given by

$$\langle \hat{H}_0(\vec{k}) \hat{H}_0(\vec{k}') \rangle_{\hat{\eta}_-} = f(\vec{k}, \vec{k}') , \quad (42)$$

where $\hat{H}_0(\vec{k}) \equiv \hat{H}_0(\vec{k}, t = 0)$, and the average has been taken over all configurations created by the noise η_- . We note that for $t > 0$, $\eta_- \equiv 0$. At $t = 0$, a new growth process with noise η is turned on. Let us denote the full

solution of the CLG equation by $\hat{H}(\vec{k}, t)$ with the initial condition $\hat{H}_0(\vec{k})$. Then,

$$\hat{H}(\vec{k}, t) = \hat{H}_0(\vec{k})e^{-a(\vec{k})t} + \hat{h}(\vec{k}, t) , \quad (43)$$

where $a(\vec{k}) \equiv \nu_1 k^2 + |\nu_2| k^4$, and $\hat{h}(\vec{k}, t)$ denotes the solution of the CLG equation with a flat initial condition. Calculating the correlation function with respect to both the old noise η_- (from $t = -t_0$ to $t = 0$) and a new noise η (for $t > 0$) gives

$$\begin{aligned} \langle \langle \hat{H}(\vec{k}, t) \hat{H}(\vec{k}', t) \rangle_{\hat{\eta}} \rangle_{\hat{\eta}_-} = \\ f(\vec{k}, \vec{k}') e^{-[a(\vec{k}) + a(\vec{k}')]t} + \langle \hat{h}(\vec{k}', t) \hat{h}(\vec{k}, t) \rangle_{\hat{\eta}} , \end{aligned} \quad (44)$$

given that either $\langle \hat{H}_0(\vec{k}) \rangle_{\hat{\eta}_-} = 0$, or $\langle \hat{h}(\vec{k}, t) \rangle_{\hat{\eta}} = 0$, which makes the crossterms disappear. The influence of the initial conditions vanishes exponentially fast in the Fourier space but not necessarily in the real space. To see this we consider the following example. At time $t = -t_0$ the surface is flat. Then we switch on the beam and let the surface evolve until $t = 0$ driven by the CLG growth dynamics (the noise η_- is white). For f we get

$$\begin{aligned} f(\vec{k}, \vec{k}') &= \langle \int_{-t_0}^0 d\tau \hat{\eta}_-(\vec{k}, \tau) e^{a(\vec{k})\tau} \int_{-t_0}^0 d\tau' \hat{\eta}_-(\vec{k}', \tau') e^{a(\vec{k}')\tau'} \rangle_{\hat{\eta}_-} \\ &= \frac{2D}{(2\pi)^d} \frac{1 - e^{-2a(\vec{k})t_0}}{2a(\vec{k})} \delta^d(\vec{k} + \vec{k}') . \end{aligned} \quad (45)$$

Integrating the first term on the right hand side of (44) with respect to \vec{k} shows that the initial roughness decays slowly, as $w_i^2 \sim t_0/t$, in the limit $t \rightarrow \infty$, when the substrate dimension $d = 2$. This corresponds precisely to (41) with EW scaling, $\xi_s \sim t_0^{1/2}$ and $\xi \sim t^{1/2}$.

In the preceding we dealt with the full CLG equation. Next we will focus on calculating the time dependent substrate surface width $w_i^2(t)$ for the special cases $\nu_2 = 0$ (EW equation, $z = 2$) and $\nu_1 = 0$ (MWV equation, $z = 4$) of (1). Moreover, we assume that the substrate surface has been grown by either EW or MWV dynamics, so that its correlations can be described by the Fourier amplitudes

$$\langle |\hat{H}_0(\vec{k})|^2 \rangle_{\hat{\eta}_-} = \frac{A_0}{k^{z_s}} [1 - e^{-(k\xi_s)^{z_s}}] \quad (46)$$

where ξ_s is the substrate correlation length, and $z_s = 2$ or $z_s = 4$ for surfaces generated by EW or MWV dynamics, respectively. The roughness exponent of the substrate is $\chi_s = (z_s - d)/2$. Solving (1) subject to the initial condition $\hat{H}_0(\vec{k})$ one obtains

$$\langle |\hat{H}(\vec{k}, t)|^2 \rangle_{\hat{\eta}} = \langle |\hat{H}_0(\vec{k})|^2 \rangle_{\hat{\eta}_-} e^{-(k\xi(t))^z} + \frac{D}{\nu} \frac{1}{k^z} [1 - e^{-(k\xi(t))^z}] \quad (47)$$

where z is the dynamic exponent of the growth process and $\xi(t) = (2\nu t)^{1/z}$ its correlation length. Since the variance w^2 is obtained by integrating (47) over k , the decomposition (40) is valid and the substrate contribution at time t is given by

$$w_i^2(t) = \Omega_{d-1} A_0 \int_0^{k_{\max}} dk k^{d-1-z_s} [1 - e^{-(k\xi_s)^{z_s}}] e^{-(k\xi)^z} . \quad (48)$$

The upper cutoff k_{\max} is of the order of the inverse lattice constant; in the following we assume that ξ_s and ξ are large compared to $1/k_{\max}$ and set $k_{\max} = \infty$ in (48).

Substituting $q = (k\xi_s)^{z_s}$ in (48) yields

$$w_i^2(t) = (\Omega_{d-1} A_0 / z_s) \xi_s^{z_s-d} \int_0^\infty dq q^{d/z_s-2} (1 - e^{-q}) e^{-\tau q^{z/z_s}} \quad (49)$$

where the dimensionless time variable $\tau = (\xi/\xi_s)^z$ has been introduced (recall that $\xi \sim t^{1/z}$). The integral can be explicitly computed if $z = z_s$; details are given in Appendix A. To analyze (49) in the general case, let us first assume that $z_s > d$, i.e. $\chi_s > 0$, which covers MWV substrates in $d = 1$ and $d = 2$, and EW substrates in $d = 1$.

This ensures that the integral over q^{d/z_s-2} converges at infinity, and hence the factor $\exp(-\tau q^{z/z_s})$ can be dropped when $\tau \ll 1$. The width is therefore independent of τ for $\tau \ll 1$. Physically this simply reflects the fact that, for a surface with power law roughness, $\chi_s > 0$, the width is dominated by the long wavelength fluctuations with wavelengths of the order of ξ_s . At time t initial fluctuations of wavelengths up to the correlation length $\xi(t)$ have been eliminated, thus the substrate contribution to the width decreases appreciably only when $\xi \approx \xi_s$ or $\tau \approx 1$.

For $z_s = d$ (i.e. $\chi_0 = 0$, for example an EW substrate in $d = 2$) the integral over q^{d/z_s-2} diverges logarithmically at large q . The factor $\exp(-\tau q^{z/z_s})$ then has to be retained, and one finds that $w_i(\tau)^2 \sim \ln(1/\tau)$ for $\tau \ll 1$; of course this behavior is valid only for $\tau > (k_{\max}\xi_s)^{-z}$, since the initial roughness $w_i(0)^2 \approx \Omega_{d-1} A_0 \ln(k_{\max}\xi_s)$. Finally, in the (somewhat academic) case $z_s < d$, $w_i(\tau)$ decreases as a power law also for $\tau \ll 1$, as $w_i(\tau)^2 \sim \xi^{-(d-z_s)}$, see Appendix A.

The behavior for large τ can be discussed independent of z_s . For $\tau \gg 1$ the integral (49) is effectively cut off at $q \approx \tau^{-z_s/z} \ll 1$, therefore we can set $1 - e^{-q} \approx q$ in the integrand, and it follows by rescaling that

$$w_i^2(\tau) \approx A_0 \xi_s^{z_s-d} (\xi_s/\xi)^d \sim t^{-d/z} . \quad (50)$$

This result has a simple interpretation. For $\xi \gg \xi_s$ the growth process averages over a large number $N = (\xi/\xi_s)^d$ of domains in which the initial fluctuations are statistically independent. The height variance of each domain is of the order $A_0 \xi_s^{z_s-d}$, and averaging over N domains reduces the variance

by a factor of $1/N$. If the substrate has power law roughness ($\chi_s > 0$), then $w_i(0)^2 \approx A_0 \xi_s^{z_s - d}$ and (50) is identical to (41).

The last argument is valid also for completely general initial conditions characterized by a correlation function of the form

$$\langle |\hat{H}_0(\vec{k})|^2 \rangle_{\hat{\eta}_-} = \frac{\Omega_{d-1} A_0}{k^{d+2\chi_0}} g(k\xi_s) \quad (51)$$

where χ_0 denotes the roughness exponent of the substrate and the scaling function $g(s)$ satisfies $g(s \rightarrow \infty) = 1$, $g(s \rightarrow 0) = 0$. The expression (49) generalizes to

$$w_i^2(\tau) = \Omega_{d-1} A_0 \xi_s^{2\chi_0} \int_0^\infty dq q^{-(1+2\chi_0)} g(q) e^{-\tau q^z}. \quad (52)$$

To extract the behavior for large τ we need to know how $g(s)$ vanishes for small s . This is fixed by requiring that (51) should have a finite limit for $k \rightarrow 0$ (this limit gives rise to the center of mass fluctuations of the surface, see [34]). Consequently $g(s) \sim s^{d+2\chi_0}$, and (52) decays as

$$w_i^2(\tau) \approx \Omega_{d-1} A_0 \xi_s^{2\chi_0} \tau^{-d/z} \approx w_i^2(0) (\xi_s/\xi)^d \quad (53)$$

in accordance with the heuristic argument.

In summary, we have shown that, under rather general conditions, the substrate contribution w_i to the width of a rough growing surface remains essentially constant as long as the correlation length ξ of the growth process is smaller than the substrate correlation length ξ_s , and that it decreases according to (41) for $\xi \gg \xi_s$. While the functional form of the transition between the two regimes is not analytically accessible in general, a useful interpolation formula is

$$w_i(t)^2 = w_i(0)^2 (1 + t/t_s)^{-d/z} \quad (54)$$

with a fit parameter t_s , which has already been employed in the analysis of experimental data [33]. In Fig. 2 the decay of the substrate width is illustrated for two special cases, and the formula (54) is compared to the exact expression derived in Appendix A.

4.2 Shape of the Height Correlation Function

The dynamic scaling hypothesis of kinetic roughening theory [21] states that the height–height correlation function should have the scaling form

$$C(x, t) \equiv \langle h(\vec{x}' + \vec{x}, t) h(\vec{x}', t) \rangle = w^2(t) F(x/\xi(t)) \quad (55)$$

with $w^2 = C(0, t)$, hence $F(0) = 1$, and $\xi \sim t^{1/z}$. To date almost all theoretical work has focused on the behavior of the height difference correlation function

$$\begin{aligned} G(x, t) &= \langle (h(\vec{x}' + \vec{x}, t) - h(\vec{x}', t))^2 \rangle \\ &= 2[C(0, t) - C(x, t)] = 2w^2[1 - F(x/\xi(t))] \end{aligned} \quad (56)$$

for $x \ll \xi$, i.e. the short distance behavior

$$F(s) \approx 1 - \mathcal{O}(s^{2\chi}) , \quad s \rightarrow 0 , \quad (57)$$

of the scaling function. In contrast, the overall shape of F or, in particular, the way it decays for large arguments has not been addressed theoretically, although a considerable amount of empirical information is available [20]. This question is of some experimental importance, since the interpretation of scattering data from rough surfaces typically requires a model for the entire correlation function [35]. A widely used form for F is [36]

$$F(s) = \exp(-s^{2\chi}) , \quad (58)$$

which assumes a simple relation between large distance and short distance behaviors. Here we show by explicit calculations within the linear theory that the large distance decay of F involves a new exponent not simply related to χ , and that moreover the decay can be oscillatory rather than monotonic. First we make some general remarks concerning the correlation function for the CLG model. The entire correlation function valid for all ranges can be rewritten for $d = 2$ as (by substitution $k' = k/\xi$ in Eq. (32))

$$G\left(\frac{x}{\xi}, \frac{\xi_1}{\xi}, \frac{\xi_2}{\xi}\right) = \frac{D}{\pi\nu_1} \frac{\xi_1^2}{\xi^2} \int_0^\infty dk k [1 - J_0(kx/\xi)] \frac{[1 - e^{-(\frac{\xi_1^2}{\xi^2}k^2 + \frac{\xi_2^4}{\xi^4}k^4)]}}{\frac{\xi_1^2}{\xi^2}k^2 + \frac{\xi_2^4}{\xi^4}k^4} , \quad (59)$$

where $\xi_1 \equiv (2\nu_1 t)^{1/2}$ and $\xi_2 \equiv (2|\nu_2|t)^{1/4}$. As far as the CLG model can be considered to describe the physics correctly either Eq. (59) or Eq. (32) could be used directly as fitting functions, with the parameters (D, ν_1, ν_2) or $(A \equiv D/(2\pi\nu_1), \xi_1, \xi_2)$ to be fitted. The amplitude is set by parameters D or A . The correlation length $\xi(t)$ in Eq. (59) corresponds to the experimentally observable correlation length. We can numerically determine the dependence of ξ on ξ_1 and ξ_2 by using the relation $C(x = \xi)/C(x = 0) = e^{-1}$, which is the usual definition of the correlation length. The surface $\xi(\xi_1, \xi_2)$ is plotted in Fig. 3. A least squarest fit for a set of solutions $\xi = \xi(\xi_1, \xi_2)$ yields

$$\xi_p \equiv \alpha_1 \xi_1 + \alpha_2 \xi_2 = 0.08533 \xi_1 + 1.60573 \xi_2 . \quad (60)$$

In addition, numerical studies show that ξ follows the scaling relation $\xi(a\xi_1, a\xi_2) = a\xi(\xi_1, \xi_2)$. Our choice $\xi_p \equiv \alpha_1 \xi_1 + \alpha_2 \xi_2$ is a simple case which quite accurately satisfies the definition for the correlation length.

Unlike in the case of the heuristic correlation function (58), the requirement $x \ll \xi$ alone is not sufficient to determine the scaling behavior of G for CLG model with a fixed exponent χ . The scaling analysis of Sec. 3 shows that the scaling of the correlation function depends on two dimensionless quantites: $\xi_1/\xi_2 \sim (t/t_c)^{1/2}$ and $\xi_1 x/\xi_2^2 \sim x/\ell^*$. If $t/t_c \gg 1$, $x/\ell^* \gg 1$, and $x \ll \xi$,

then $G \propto x^{2\chi_1(d=2)}$ and $\chi \approx \chi_1(d=2) = 0$. If $t/t_c \ll 1$, $x/\ell^* \ll 1$, and $x \ll \xi$, then $G \propto x^{2\chi_2(d=2)} \ln(\xi_2/x)$ and thus $\chi \approx \chi_2(d=2) = 1$.

Let us next determine the behavior of the correlation function for large values of the ratio $x/\xi \equiv s$. Rather than trying to present the full solution for the CLG model we shall limit ourselves to the one and two dimensional EW and MWV models. For the $d = 1$ EW case, the evaluation of C is straightforward. We have

$$\partial_t C(x, t) = \frac{2Ds}{\pi x} \int_0^\infty dk e^{iks-k^2} . \quad (61)$$

This is a Gaussian integral which can be done. The integration over t is also standard. We obtain the result:

$$C(x, t) = w^2(t) F(s) , \quad (62)$$

with

$$w^2(t) = \frac{D\xi_1}{\nu_1\sqrt{\pi}} ; \quad (63)$$

$$F(s) = \frac{1}{2} \int_0^1 dy y^{-1/2} e^{-s^2/(4y)} \rightarrow 2s^{-2} e^{-s^2/4} \quad (64)$$

as $s \rightarrow \infty$. The behavior of the scaling function F is in striking contradiction to the conventional ansatz (58), which would lead one to expect an exponential decay for $\chi = 1/2$.

The $d = 2$ EW case is also simple to calculate:

$$\partial_t C(x, t) = \frac{D}{\pi} \int_0^\infty dk k J_0(kx) e^{-(\xi_1 k)^2} . \quad (65)$$

Integrating the result from 0 to t yields [13]

$$C(s) = \frac{D}{4\pi\nu_1} \int_{s^2/4}^\infty dy y^{-1} e^{-y} \equiv \frac{D}{4\pi\nu_1} E_1(s^2/4) , \quad (66)$$

where E_1 is an exponential integral. The asymptotic power law expansion of E_1 reveals that as a function of s the leading term is equivalent to the $d = 1$ case: $E_1(x) \sim x^{-1} e^{-x} (1 - x^{-1} + 2x^{-2} - \dots)$, hence $F(s) \sim s^{-2} e^{-s^2/4}$. In the $d = 1$ MWV case we confront the integral [37]

$$\partial_t C(x, t) \propto \xi_2^{-1} \int_{-\infty}^\infty dk e^{isk-k^4} \equiv \xi_2^{-1} \int_{-\infty}^\infty dk e^{-f(k)} . \quad (67)$$

The behavior of the leading asymptotic behavior can be evaluated using the method of stationary phase [38]. In the limit $s \rightarrow \infty$ only the neighborhoods of saddle points contribute to the integral. They are determined from the relation $\partial_k f = 0$:

$$k_0 \equiv \left(\frac{s}{4}\right)^{1/3} e^{i\pi/6} , \quad k_1 \equiv \left(\frac{s}{4}\right)^{1/3} e^{i5\pi/6} , \quad k_2 \equiv \left(\frac{s}{4}\right)^{1/3} e^{i3\pi/2} . \quad (68)$$

Removal of each saddle point to the origin results in a quadratic dependence of $f(k)$ on k : $f(k) - f(k_i) \rightarrow b_i k^2$ as $k \rightarrow 0$, $i = 0, 1, 2$. Thus, in the leading approximation we retain only the Gaussian part of the integrand:

$$\partial_t C(x, t) \propto \xi_2^{-1} b_i^{-1/2} e^{-f(k_i)} . \quad (69)$$

Furthermore, we note that the contributions coming from distinct saddle points are additive if the paths of integration are properly chosen in the complex plane. Despite that the individual contributions coming from points k_0 and k_1 are complex, their sum is real. The point k_2 has to be discarded as it would cause an exponential blow-up. Finally, we obtain

$$C(x, t) \sim \frac{\xi_2^3}{|\nu_2|} s^{-5/3} e^{-a_1 s^{4/3}} [a_1 \sin(a_2 s^{4/3}) + a_2 \cos(a_2 s^{4/3})] , \quad (70)$$

where $a_1 \equiv (3/8)4^{-1/3}$ and $a_2 \equiv (3\sqrt{3}/8)4^{-1/3}$. The correlation function C is an oscillating function for large values of the argument s and can assume negative values as well.

For the $d = 2$ MWV case we use the same method as in the previous case:

$$\partial_t C(x, t) = \frac{2D}{(2\pi)^2} \int_{-\infty}^{\infty} dk_1 \int_{-\infty}^{\infty} dk_2 e^{-2\xi_2^4(k_1^2+k_2^2)^2 + i(k_1 x_1 + k_2 x_2)} . \quad (71)$$

To determine the saddle points we set $\partial_{k_1} f = \partial_{k_2} f = 0$, where f denotes the expression in the exponential of (71). This yields

$$\partial_{k_1} f = 0 \quad ; \quad \partial_{k_2} f = 0 , \quad (72)$$

$$\Rightarrow 4\xi_2^4 k_1^3 + 4\xi_2^4 k_1 k_2^2 - i x_1 = 0 \quad ; \quad 4\xi_2^4 k_2^3 + 4\xi_2^4 k_2 k_1^2 - i x_2 = 0 , \quad (73)$$

which can be solved with the ansatz $k_1 = a x_1$, $k_2 = a x_2$. Again we get three saddle points, one of which corresponds to an exponential divergence. Summing up the contributions of the remaining two and integrating over time gives a real answer:

$$C(s) \sim \frac{\xi_2^2}{|\nu_2|} s^{-2} e^{-a_1 s^{4/3}} \cos(a_2 s^{4/3}) . \quad (74)$$

As before, an oscillating function results.

Summarizing, it appears that the large distance decay of the scaling function $F(s)$ in (55) generally has the form of a ‘squeezed’ exponential decorated by a subleading power law,

$$F(s) \approx s^{-\gamma} e^{-c s^\delta} , \quad s \rightarrow \infty , \quad (75)$$

where the amplitude c can be real (as in the EW equation) or complex (as in the MWV equation); in the latter case the decay is modulated by oscillations. In contrast to what is suggested by the heuristic function (58),

the decay exponent has no direct relation to the roughness exponent χ ; rather, in the examples treated here, δ seems to be characteristic of the surface relaxation process but independent of dimensionality. In Appendix B we give an alternative derivation for $d = 1$ which suggests that $\delta = z/(z - 1)$ and $\gamma = 1 + \delta/2$ for the generalized linear equation

$$\partial_t h = -(-\partial_x^2)^{z/2} h + \eta \quad (76)$$

with integer values of $z/2$.

It is worth pointing out that a rapid, exponential-like decay of the correlation function should be expected only for growth processes that are *local* in space, such as (76), for which the Fourier transform of $C(\vec{x}, t)$ is an analytic function of \vec{k} for small $|\vec{k}|$. A simple example of a nonlocal kinetic roughening process is diffusion limited erosion [39], formally the generalization of (76) to $z = 1$, for which it can be shown that in $d = 1$

$$C(x, t) = \frac{1}{2\pi} \frac{D}{\nu} \ln(1 + \xi^2/x^2) \quad (77)$$

for distances larger than the lattice spacing a ; at $x \approx a$, $C \approx w^2 \approx (D/\nu) \ln(\xi/a)$, since $\chi = (1 - d)/2 = 0$ in $d = 1$ [39]. As usual, the correlation length is $\xi = 2\nu t$. At large distances (77) decays as a power law, $C \sim (\xi/x)^2$, reflecting the nonlocal nature of the interface dynamics.

4.3 Effects of Noise

We have shown in Sec. 2 that the correlation function for the noise typically consists of two components,

$$\langle \eta(\vec{x}, t) \eta(\vec{x}', t') \rangle = 2(D_1 - D_2 \nabla^2) \delta(\vec{x} - \vec{x}') \delta(t - t') \quad (78)$$

where the first, white noise component arises from evaporation and deposition, while the second, conserved component reflects the thermal fluctuations in the surface current [8]. In Fourier space the correlator (78) reads

$$\langle \tilde{\eta}(\vec{k}, \omega) \tilde{\eta}(\vec{k}', \omega') \rangle_{\tilde{\eta}} = (2\pi)^{-d} (2D_1 + 2D_2 k^2) \delta^d(\vec{k} + \vec{k}') \delta(\omega + \omega') , \quad (79)$$

where $\tilde{\eta}$ denotes the Fourier transform with respect to both space and time. So far we have considered the behavior of the surface on scales large compared to the noise crossover scale $\ell^{**} \sim (D_2/D_1)^{1/2}$, where the conserved part can be neglected. In the opposite regime $x \ll \ell^{**}$ we can set $D_1 = 0$ and analyze the behavior generated only by diffusion noise. The corresponding power laws are easily evaluated: Because the D_2 correlator in (79) is of the same form as for the white noise apart from the factor k^2 , the results presented in Sec. 3 hold if we replace d by $d + 2$.

In Ref. [41] it was pointed out that the effect of fast degrees of freedom may sometimes be represented by means of a coloured noise term η_c , i.e. the noise

has power law correlations. Through renormalization group analysis it was shown that power law correlated noise changes the scaling exponents for the KPZ equation. Now we shall extend our analysis of Eq. (1) to include power law correlated noise as well. We assume that the noise has long distance correlations of the form

$$\langle \eta_c(\vec{x}, t) \eta_c(\vec{x}', t') \rangle_{\eta_c} = |\vec{x} - \vec{x}'|^{2\rho-d} |t - t'|^{2\varrho-1} , \quad (80)$$

with $0 < \rho < d/2$ and $0 < \varrho < 1/2$. Taking the Fourier transform of Eq. (80) leads to

$$\langle \tilde{\eta}_c(\vec{k}, \omega) \tilde{\eta}_c(\vec{k}', \omega') \rangle_{\tilde{\eta}} = \frac{2D(k, \omega)}{(2\pi)^d} \delta^d(\vec{k} + \vec{k}') \delta(\omega + \omega') , \quad (81)$$

where $D(k, \omega) = D'|\vec{k}|^{-2\rho}|\omega|^{-2\varrho}$, and D' is a function of ρ and ϱ . The analysis of the power law behavior for both EW and MWV cases we get the following relations between the new roughening exponents (primed) and the old ones:

$$\beta'_1 = \beta_1 + \frac{1}{2}\rho + \varrho \quad ; \quad \chi'_1 = \chi_1 + \rho + 2\varrho . \quad (82)$$

$$\beta'_2 = \beta_2 + \frac{1}{4}\rho + \varrho \quad ; \quad \chi'_2 = \chi_2 + \rho + 4\varrho . \quad (83)$$

Clearly, $z'_1 \equiv \chi'_1/\beta'_1 = 2$ and $z'_2 \equiv \chi'_2/\beta'_2 = 4$ are satisfied because $\chi_1/\beta_1 = 2$ and $\chi_2/\beta_2 = 4$. These results agree with previous treatments [12, 16, 41].

5 Summary and Conclusions

In this work, we have presented a detailed quantitative analysis of a combined linear stochastic growth equation, which incorporates both EW and MWV type of behavior. In particular, we have identified the relevant scaling variables and calculated in detail the behavior of the surface width, and various correlation functions in different regimes. Our analysis shows that the CLG model possesses MWV type of scaling regime at early times ($t \ll t_c$) and crosses over to EW type of growth for later times. In a finite system it is, however, possible that the system maintains MWV type of growth dynamics for all times given that the prefactor of the fourth order gradient term is very large ($L \ll \ell^*$). Additionally, the equal time and saturated correlation functions reveal interesting and complicated crossover behavior between the two limits. We should also note that in the appropriate limits, our results completely agree with the previously derived results for concerning the surface width and the equal time correlation functions of the EW and MWV equations [4, 12, 13, 14, 15, 16]. We have also recalculated the scaling exponents in Sec. 4 for coloured noise that has long range spatial and temporal correlations. Our results show that the long-range part of the

noise changes the exponents, in analogy to the case of the nonlinear KPZ equation [41].

The solvability of the CLG model allows us to address other important problems related to surface growth problems as well. A particularly interesting case concerns the influence of rough initial conditions. In Sec. 4 we demonstrate that the effect of initial roughness in $d = 2$ disappears as a power law in time $\sim t_0/t$ if the surface has initially roughened through the CLG growth dynamics for a time t_0 . In general, the initial roughness vanishes as $(\xi_s/\xi)^d \sim t^{-d/z}$ for EW and MWV models as $\xi \gg \xi_s$. For a general growth process the behavior of this transient is easy to evaluate by Fourier transforming the exponentially damped initial height–height correlation function (Eq. (44)).

Finally, to make the connection to experiments more concrete we have proposed the use of the parametrized correlation functions obtained for the CLG model for fitting of diffusive x-ray reflectivity data. In Sec. 4 we establish a relation between the parameters ν_1 and ν_2 of the CLG growth model and the experimental fitting parameter ξ (cf. Eq. (60)). Moreover, both the small ($x \ll \xi$) and the large ($x \gg \xi$) scale behavior of the correlation function of the CLG model are found to be different from the experimentally used fitting functions. This also implies that the measured decay exponent χ from heuristic fitting functions bear no direct relation to the roughness exponent of the CLG model. We hope that these calculations will be useful in future experiments on surface growth.

Acknowledgements: J. K. wishes to thank H. T. Dobbs, M. Funke and F. König for stimulating discussions. This work has in part been supported by a joint grant between the Academy of Finland, and Deutscher Akademischer Austauschdienst.

E-mail addresses: `majaniemi@fltxa.helsinki.fi`, `ala@fltxa.helsinki.fi`,
`j.krug@kfa-juelich.de`

Appendix A: Substrate Roughness for $z_s = z$

Here we explicitly evaluate the integral (49) in the special case $z_s = z$. Taking the derivative of (49) with respect to τ and reintegrating we obtain

$$w_i^2 = \frac{\Omega_{d-1} A_0 \Gamma(d/z)}{z-d} \xi_s^{z-d} [(\tau+1)^{1-d/z} - \tau^{1-d/z}]. \quad (84)$$

Three cases have to be distinguished.

(i) $z > d$: In this case both the substrate and the growing surface are rough with roughness exponent $\chi = (z-d)/2 > 0$. The expression (84) then has a finite limit $w_i^2(0) = \Omega_{d-1} A_0 \Gamma(d/z) \xi_s^{z-d}/(z-d)$ for $\tau \rightarrow 0$. For $\tau \ll 1$ the roughness remains essentially unchanged,

$$w_i(\tau)^2 \approx w_i(0)^2 (1 - \tau^{1-d/z}), \quad (85)$$

while for $\tau \gg 1$ it decays as

$$w_i^2(\tau) \approx (1 - d/z) w_i^2(0) \tau^{-d/z} \quad (86)$$

in accordance with (41).

(ii) $z = d$: Substrate and surface are logarithmically rough. Taking the limit $(z-d) \rightarrow 0$ in (84) gives

$$w_i^2(\tau) = (\Omega_{d-1} A_0 / z) \ln(1 + 1/\tau) \quad (87)$$

which diverges for $\tau \rightarrow 0$. Clearly (87) is valid only for $\xi > k_{\max}^{-1}$, i.e. $\tau > \tau_0 = (k_{\max} \xi_s)^{-z}$; the initial roughness is $w_i(\tau_0)^2 \approx \Omega_{d-1} A_0 \ln(k_{\max} \xi_s)$. For $\tau_0 \ll \tau \ll 1$ the substrate contribution decays slowly, as $w_i(\tau)^2 \approx \Omega_{d-1} A_0 \ln(1/\tau)$, while for $\tau \gg 1$ (87) reduces to

$$w_i^2(\tau) \approx (\Omega_{d-1} A_0 / z) \tau^{-1} \quad (88)$$

which is of the form (41) with a prefactor of order unity.

(iii) $z < d$: Substrate and surface are smooth, and the width is microscopic at all times. In this case (84) combines two power law decays: For $\tau \ll 1$

$$w_i^2(\tau) \sim \xi_s^{-(d-z)} \tau^{-(d/z-1)} \sim \xi^{-(d-z)} \quad (89)$$

independent of ξ_s , while for $\tau \gg 1$ one finds

$$w_i^2(\tau) \approx [\Omega_{d-1} A_0 \Gamma(d/z)/z] \xi_s^{-(d-z)} \tau^{-d/z} \sim \xi_s^{-(d-z)} (\xi_s/\xi)^d \quad (90)$$

as in the previous two cases.

Appendix B: Derivation of the Exponent δ

Here we present a simple way of computing the exponents δ and γ characterizing the decay of the height correlation scaling function (75) for the generalized linear equation (76) in one dimension. It follows immediately from (76) that the Fourier transform $\hat{F}(q)$ of $F(s)$ is, up to some factor,

$$\hat{F}(q) \approx q^{-z}(1 - e^{-q^z}). \quad (91)$$

We now exploit the fact that by definition, $\hat{F}(q)$ can also be written as [40]

$$\hat{F}(q) \approx \sum_{n=0}^{\infty} \frac{A_n}{n!} (-iq)^n \quad (92)$$

where

$$A_n = \int_{-\infty}^{\infty} ds s^n F(s) \quad (93)$$

is the n^{th} moment of the real space scaling function. Comparing (91) to the power series (92), we obtain the relation

$$|A_{zk}| \approx \frac{1}{k+1} \frac{(zk)!}{k!}, \quad k = 0, 1, 2, \dots \quad (94)$$

The asymptotics of $F(s)$ can then be extracted by comparing the behavior of (94) for large k with that obtained from the ansatz (75) inserted into (93); assuming the amplitude c in (75) to be real, the integral (93) is easily evaluated in the saddle point approximation. The leading behavior is $A_n \sim n^{n/\delta}$ which, compared to $|A_{zk}| \sim k^{(z-1)k}$ from (94), implies that $\delta = z/(z-1)$. Moreover, from the integral (93) one obtains a power law factor $\sim n^{1/\delta-1/2-\gamma/\delta}$ which has to be matched to the factor $(k+1)^{-1}$ that appears in (94); this forces γ to take the value $\gamma = 1 + \delta/2$. Both results agree with the detailed calculations of Sec. 4.2.

References

- [1] *Dynamics of Curved Fronts*, ed. P. Pelcé (Academic Press, London 1988).
- [2] M. Kardar, G. Parisi and Y.-C. Zhang, Phys. Rev. Lett. **56**, 889 (1986).
- [3] N. Provatas, T. Ala-Nissila, M. Grant, K. R. Elder, and L. Piché, Phys. Rev. E **51**, 4232 (1995).
- [4] S. F. Edwards and D. R. Wilkinson, Proc. R. Soc. Lond. A **381**, 17 (1982).
- [5] D. E. Wolf and J. Villain, Europhys. Lett. **13**, 389 (1990).
- [6] S. Das Sarma and P. Tamborenea, Phys. Rev. Lett. **66**, 325 (1991).
- [7] L. Golubović and R. Bruinsma, Phys. Rev. Lett. **66**, 321 (1991).
- [8] J. Villain, J. Phys. I **1**, 19 (1991).
- [9] A. Zangwill, C. N. Luse, D. D. Vvedensky and M. R. Wilby, Surf. Sci. Lett. **274**, 529 (1992); C. N. Luse, A. Zangwill, D. D. Vvedensky and M. R. Wilby, *ibid.* 535; C. N. Luse and A. Zangwill, Phys. Rev. B **48**, 1970 (1993).
- [10] D. D. Vvedensky, A. Zangwill, C. N. Luse and M. R. Wilby, Phys. Rev. E **48**, 852 (1993).
- [11] F. Family, J. Phys. A **19**, L441 (1986).
- [12] P.-M. Lam and F. Family, Phys. Rev. A **44**, 4854 (1991).
- [13] T. Nattermann and L.-H. Tang, Phys. Rev. A **45**, 7156 (1992).
- [14] J. Amar, P.-M. Lam and F. Family, Phys. Rev. E **47**, 3242 (1993).
- [15] S. Das Sarma, S. V. Ghaisas and J. M. Kim, Phys. Rev. E **49**, 122 (1994).
- [16] Y.-K. Yu, N.-N. Pang and T. Halpin-Healy, Phys. Rev. E **50**, 5111 (1994).
- [17] W. W. Mullins, “Solid surface morphologies governed by capillarity”, in *Metal Surfaces: Structure, Energetics and Kinetics*, N.A. Gjostein and W.D. Robertson, eds. (American Society of Metals, Metals Park 1963).
- [18] G. Palasantzas, Phys. Rev. B **49**, 10544 (1994).

- [19] J. Villain, A. Pimpinelli, L. Tang and D. Wolf, J. Phys. I France **2**, 2107 (1992).
- [20] W. M. Tong and R. S. Williams, Annu. Rev. Phys. Chem. **45**, 401 (1994).
- [21] Recent reviews are P. Meakin, Phys. Rep. **235**, 189 (1993); T. Halpin-Healy and Y. C. Zhang, *ibid.* **254**, 215 (1995); A.-L. Barabási and H. E. Stanley, *Fractal Concepts in Surface Growth* (Cambridge University Press, Cambridge 1995); J. Krug, in *Scale Invariance, Interfaces and Non-Equilibrium Dynamics*, eds. A. J. McKane, M. Droz, J. Vanimetus and D. E. Wolf (Plenum Press, 1995) p. 1. For a survey of experimental work see J. Krim and G. Palasantzas, Int. J. Mod. Phys. B **9**, 599 (1995) and also [20].
- [22] J.D. Weeks, “The roughening transition”, in *Ordering in strongly fluctuating condensed matter systems*, T. Riste, ed. (Plenum Press, New York 1980).
- [23] J. Krug, H. T. Dobbs and S. Majaniemi, Z. Phys. B **97**, 281 (1995).
- [24] J. Krug, M. Plischke, and M. Siegert, Phys. Rev. Lett. **70**, 3271 (1993).
- [25] R. L. Schwoebel and E. J. Shipsey, J. Appl. Phys. **37**, 3682 (1966); R. L. Schwoebel, J. Appl. Phys. **40**, 614 (1969).
- [26] J. Krug and M. Schimschak, J. Phys. France I **5**, 1065 (1995).
- [27] Z. L. Liao and H. J. Zeiger, J. Appl. Phys. **67**, 2434 (1990).
- [28] M. Schroeder, M. Siegert, D. E. Wolf, J. D. Shore and M. Plischke, Europhys. Lett. **24**, 563 (1993).
- [29] J. Krug, Phys. Rev. Lett. **72**, 2907 (1994).
- [30] C. Thompson, G. Palasantzas, Y. P. Feng, S. K. Sinha and J. Krim, Phys. Rev. B **49**, 4902 (1994); G. Palasantzas and J. Krim, Phys. Rev. Lett. **73**, 3564 (1994).
- [31] T. Salditt, T. H. Metzger and J. Peisl, Phys. Rev. Lett. **73**, 2228 (1994); D. G. Stearns, J. Appl. Phys. **71**, 4286 (1992); E. Spiller, D. Stearns and M. Krumrey, *ibid.* **74**, 107 (1993).
- [32] U. Klemradt, M. Funke, M. Fromm, B. Lengeler, J. Peisl and A. Förster, to appear in Physica B.
- [33] F. König, PhD Dissertation (Jülich Report Nr. 3092, 1995).
- [34] J. Krug, Phys. Rev. A **44**, R801 (1991).

- [35] G. Palasantzas and J. Krim, Phys. Rev. B **48**, 2873 (1993).
- [36] S. K. Sinha, E. B. Sirota, S. Garoff and H. B. Stanley, Phys. Rev. B **38**, 2297 (1988); W. Weber and B. Lenglens, Phys. Rev. B **46**, 7953 (1992); for a review see S. K. Sinha, J. Phys. III France **4**, 1543 (1994).
- [37] P. Collet, F. Dunlop and T. Gobron, J. Stat. Phys. **79**, 215 (1995).
- [38] R. B. Dingle, *Asymptotic Expansions: Their Derivation and Interpretation* (Academic Press 1973).
- [39] J. Krug and P. Meakin, Phys. Rev. Lett. **66**, 703 (1991).
- [40] This expansion was proposed to us by H. T. Dobbs.
- [41] E. Medina, T. Hwa, M. Kardar and Y.-C. Zhang, Phys. Rev. A **39**, 3053 (1989).

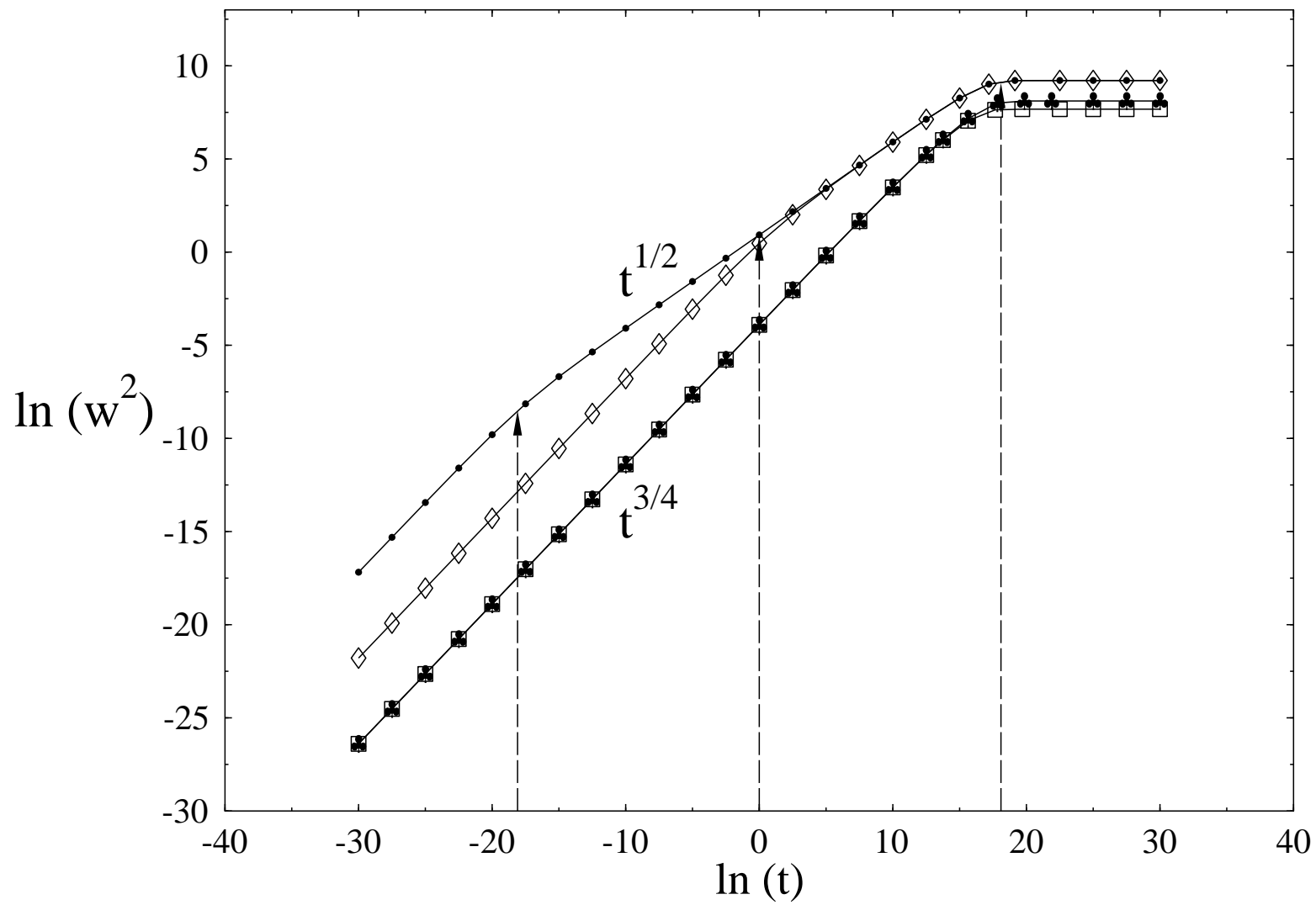
Figure Captions

Fig. 1 A log-log plot of the surface width $w^2(t)$ of the CLG equation for several values $|\nu_2|$ and ν_1 in $d = 1$, with $L = 10000$. The two scaling regimes of the surface width $w^2 \propto t^{3/4}$ for $t \ll t_c$ and $w^2 \propto t^{1/2}$ for $t \gg t_c$ are clearly visible. For the topmost curve $\nu_1 = 1$ and $|\nu_2| = 10^{-8}$ and the crossover time $\ln t_c \equiv \ln(|\nu_2|/\nu_1^2) \approx -18$ is shown. For the second curve $\nu_1 = |\nu_2| = 1$, and $\ln t_c = 0$. Finally, the two overlapping lowest curves represent the CLG surface width with $\nu_1 = 1$ and $|\nu_2| = 10^8$, and the pure MWV case with $\nu_1 = 0$, $|\nu_2| = 10^8$. In both cases the saturation time $\ln t_s \approx 18$.

Fig. 2 Decay of the substrate contribution to the surface width for dimensionality $d = 2$ and dynamic exponents $z_s = z = 4$ (full upper curve) and $z_s = z = 2$ (full lower curve). The full curves show the exact expressions derived in Appendix B, while the dotted curve shows the interpolation formula (54). The dashed lines indicate the asymptotic power laws.

Fig. 3 (a) The correlation length ξ as a function of the two dynamical correlation lengths $\xi_1 \equiv (2\nu_1 t)^{1/2}$ and $\xi_2 \equiv (2|\nu_2| t)^{1/4}$ of the CLG model. (b) The relative error $E \equiv (\xi_p - \xi)/\xi$ between the plane fit $\xi_p = \alpha_1 \xi_1 + \alpha_2 \xi_2$ and ξ (Eq. (59)). The *average* relative error is about 1%. The maximum error in the figure (10%) occurs for large ξ_1 and small ξ_2 .

Figure 1: (Majaniemi, Ala-Nissila, Krug)



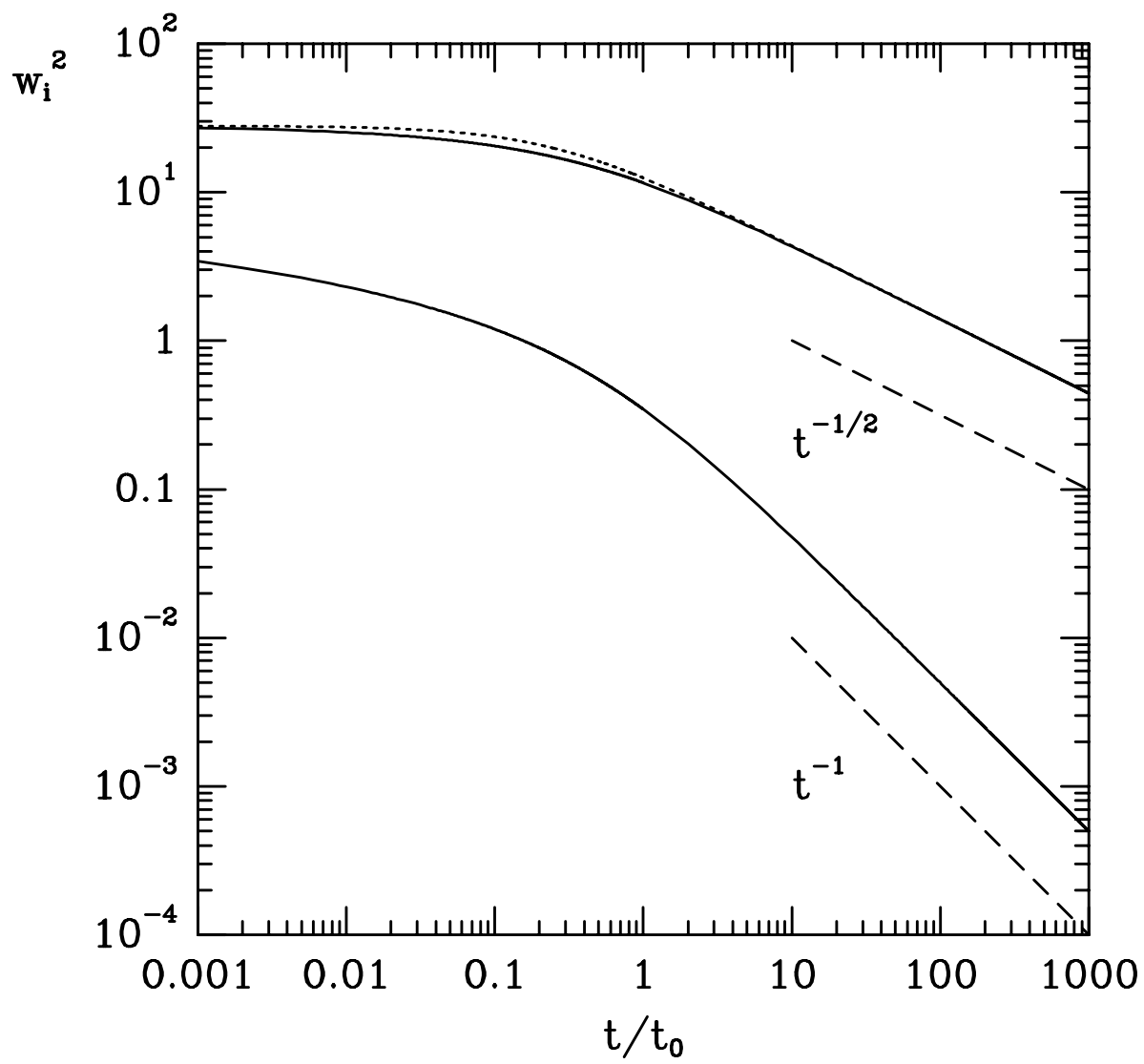


Figure 2: (Majaniemi, Ala-Nissila, Krug)

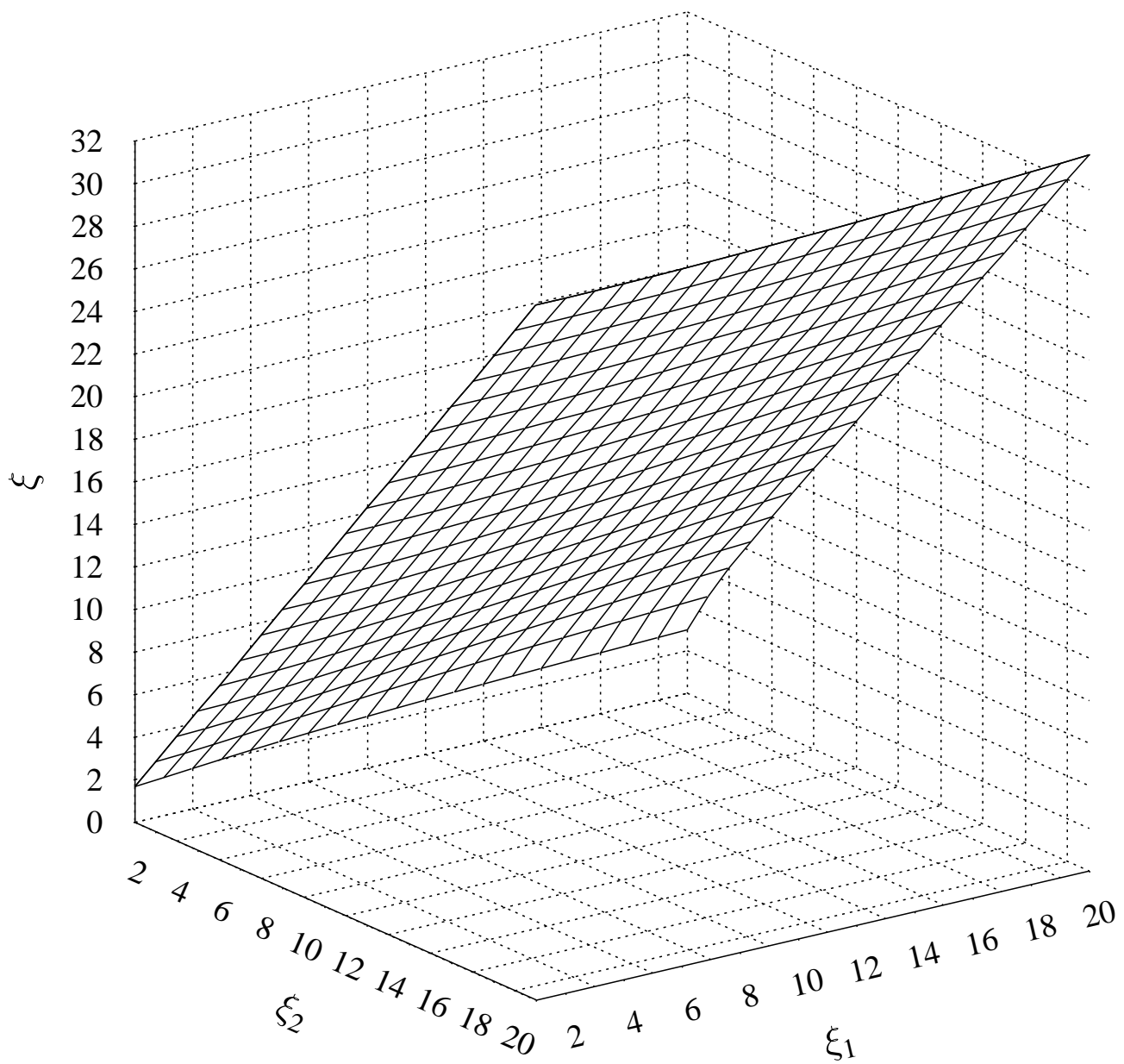


Figure 3: (a) (Majaniemi, Ala-Nissila, Krug)

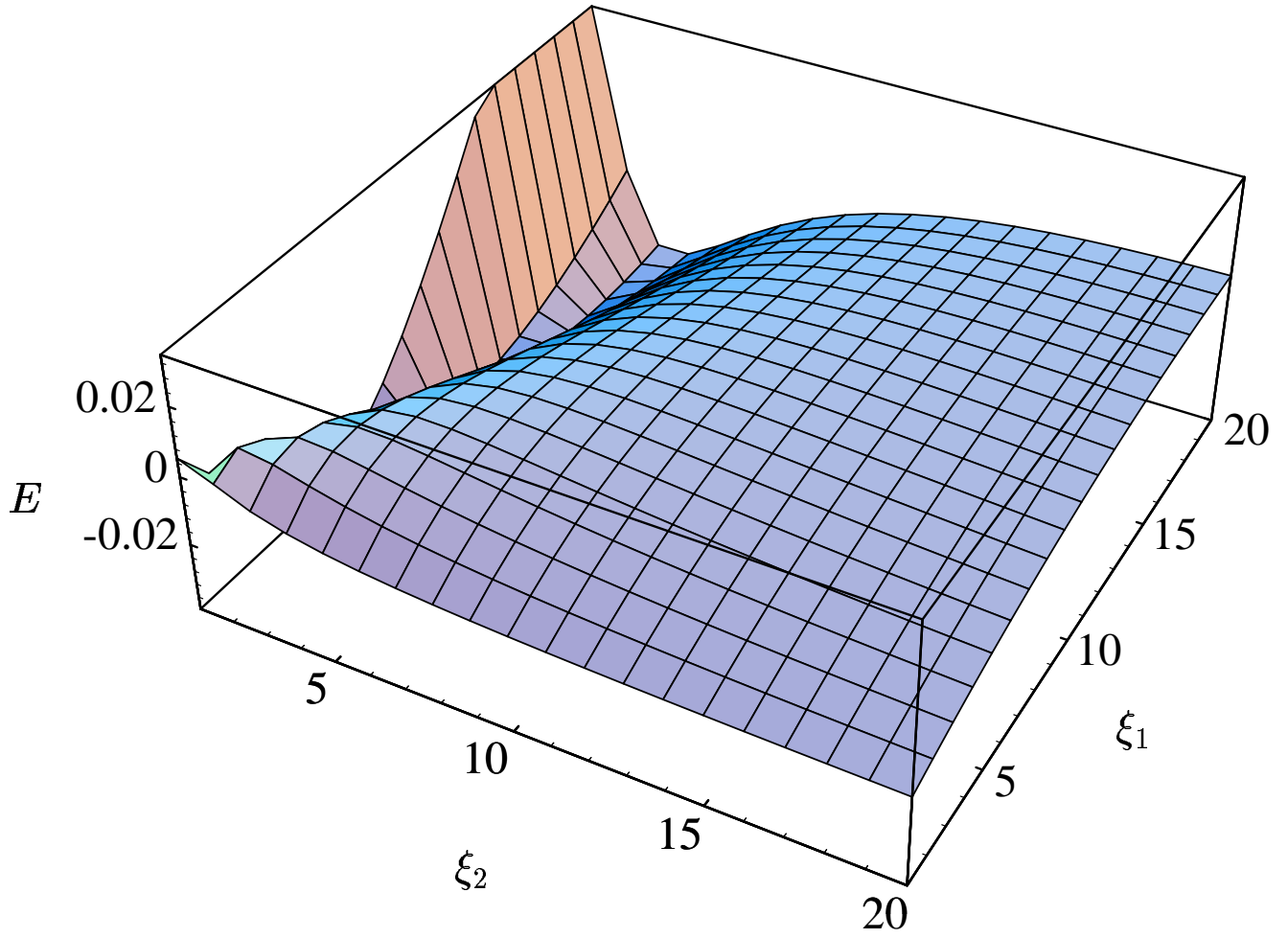


Figure 3: (b) (Majaniemi, Ala-Nissila, Krug)